of the transitions 25 $b_g\downarrow \rightarrow$ 32 $b_u\downarrow$ and 32 $b_u\downarrow \rightarrow$ 29 $b_g\downarrow$ (Table V) and owes its intensity to d–d component transitions on Pt(1) and Pt(2).

There remain to be assigned two very weak absorptions: an x-polarized band at 550 nm and a feature of unknown polarization at ~800 nm (diffuse reflectance spectrum). Only one dipole-allowed transition below 3.0 eV has not been accounted for; we assign the ~800-nm feature to this transition since it is in good agreement with the predicted energy (Table V).[27] The 550-nm band must be attributed to dipole-forbidden vibronically allowed transitions. There are three transitions of this type which are in good agreement with the observed energy (Table V). Since the 550-nm band is observed only below 30 K, the vibronic coupling presumably occurs in the excited state and causes its symmetry to become ^2B_g. Mixing of this state with the nearby ^2B_g state associated with the 26 $b_g\downarrow \rightarrow$ 32 $b_u\downarrow$ transition transfers intensity from the 460-nm dipole-allowed ligand-to-metal charge-transfer band to the 550-nm band.

Discussion of Other Spectroscopic Results and Chemical Behavior. XPS,[5b] ESR,[5c,d] and the present single-crystal optical spectroscopic measurements indicate that the unpaired spin in *cis*-diammineplatinum α-pyridone blue is in a d_{z^2}-like molecular orbital delocalized over the Pt chain. This conclusion is confirmed by the Xα calculation which shows the PPB HOMO to be delocalized over all four Pt atoms and to be comprised of overlapping $d_{z^2}^-$, d_{yz}^-, p_z^+ hybrid orbitals on Pt(1) and $d_{z^2}^-$, s^- hybrid orbitals on Pt(2). Of the unpaired spin density 91% is contained within the Pt spheres, with 41% in 2 Pt(1) and 50% in 2 Pt(2). PPB is evidently a Robin–Day class III-A compound.[28,29]

Since the Xα calculation has provided a description of the valence MO's of PPB, we can now rationalize certain aspects of its behavior and point out some interesting possibilities which have not yet been realized. Addition of an electron to the σ^* LUMO is expected to cancel the Pt(2)–Pt(2) bond. This expectation is realized through the observation that the one-electron reduction product of PPB is a Pt(II) dimer which associates in the solid state to a tetramer with a nonbonding Pt(2)–Pt(2) interaction.[23] Electron donation by axial ligands and excitation by light can also increase the electron density in the LUMO and promote dissociation of the Pt(2.25) tetramer to dimers. The effectiveness of donor anions in causing the dissociation of the tetramer has been observed,[5d] but the effect of light has not been studied. Removal of an electron from the PPB HOMO is expected to increase the strength of both Pt(1)–Pt(2) and Pt(2)–Pt(2) bonding. A one-electron oxidation of PPB should therefore lead to a Pt(2.5) tetramer. This species has not yet been observed since in the experiments where oxidation was carried out it is likely that the tetramer was largely predissociated.[23] A tetranuclear Pt(2.5) α-pyridone analogue, $[Pt(NH_3)_2(C_4H_6NO)]_4^{6+}$ (C_4H_6NO = α-pyrrolidonate), is known,[3d] however, and has Pt–Pt distances of 2.70 Å, ca. 0.15 Å shorter than in PPB. Further successive one-electron oxidations of a Pt(2.5) tetramer to Pt(2.75) and Pt(III) tetramers would also appear to be possible. The electrons for these oxidations would be removed from orbital 32 a_g. Since orbital 32 a_g does not show metal–metal interaction but is Pt–pyridone oxygen π^* in character, it is expected that Pt(2.5), Pt(2.75), and Pt(III) tetramers would all have similar metal–metal bonding but that the Pt(2.75) and Pt(III) complexes would have slightly shorter Pt–pyridone oxygen bonds.[30]

Acknowledgment. This work was supported by PHS Grants CA 15826 (at Columbia University) and CA 34992 (at MIT) awarded by the National Cancer Institute (to S.J.L.), DHHS, and at the University of Kentucky by a grant from the Research Corporation (to P.E.F.). We thank Engelhard Industries for a generous loan of K_2PtCl_4 from which the platinum compound was synthesized.

Registry No. PPB, 62782-86-9.

Supplementary Material Available: Table S1 reporting the atomic coordinates, sphere radii, and α values used in the calculation, Tables S2–S3 reporting valence and core levels, and Table S4 reporting virtual levels (18 pages).

(26) Some of the intensity underlying the 460-nm (x) band must be due to the forbidden x component of the 480-nm (y,z) band, which should become manifest by the same mechanisms discussed earlier for the x component of the 680-nm (y,z) band. It is unlikely that this could account for more than half of the observed intensity.

(27) It may be that the ~800-nm feature is an artifact and that the 27 $b_g\downarrow \rightarrow$ 32 $b_u\downarrow$ transition is not observed. We reject assigning this transition to the 550-nm band because of the large discrepancy between calculated and observed energy.

(28) Robin, M. B.; Day, P. *Adv. Inorg. Chem. Radiochem.* **1967**, *10*, 247.

(29) Wong, K. Y.; Schatz, P. N. *Prog. Inorg. Chem.* **1981**, *28*, 369.

(30) *cis*-Diammineplatinum(III) dimers with bridging α-pyridonate ligands have Pt–O distances[23] of 1.991–2.007 Å compared to 2.016 and 2.022 Å in PPB.

Theoretical Study of Dimeric Forms of Ground-State Benzene Molecules[1a]

Ray Engelke, P. Jeffrey Hay,* Daniel A. Kleier,[1b] and Willard R. Wadt

Contribution from Los Alamos National Laboratory, Los Alamos, New Mexico 87545.
Received October 20, 1983

Abstract: The relative energies and interconversion barriers of four chemically bound dimeric forms of benzene—*p,p'*-dibenzene (**2**), hexaprismane (**3**), and *exo*- and *endo*-*o,o'*-dibenzene (**4** and **5**)—are examined by using semiempirical MNDO calculations, ab initio GVB–CI techniques, and thermochemical group-additivity methods. We conclude from the calculations that the relative energies of these species are **3** > **4**, **5** > **2** > two benzene molecules (**1**). The species **2** and **3** are metastable along D_{2h} pathways; the decomposition **2** → **1** is also found to have a large energy barrier along a C_{2v} pathway. Similar conclusions are found for the reactions **4** → **1** and **5** → **1** along C_{2h} and C_{2v} paths. Of the species examined only **5** has been observed in the laboratory. Previous efforts to produce the dimers experimentally are briefly discussed.

Of the various chemically bound $(CH)_{12}$ isomers that could be formed from two ground-state benzene molecules (**1**), possibilities include the *p,p'*-dibenzene (**2**) and *o,o'*-dibenzene (**4** and **5**) species and the highly strained hexaprismane (**3**) molecule. Of these

0002-7863/84/1506-5439$01.50/0

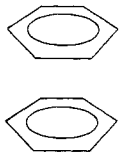

1

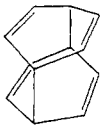

2

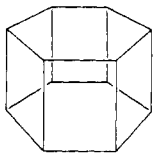

3

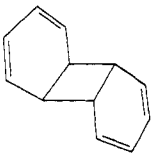

4

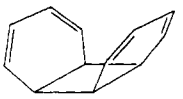

5

only **5** appears to have been synthesized to date. In this study we present the results of semiempirical and *ab initio* quantum mechanical calculations as well as thermochemical calculations on these species. The relative stabilities of these molecules and their barriers to decomposition into two benzene molecules are investigated. We examine concerted formation of **2**, **4**, or **5** from **1**; such reactions are Woodward–Hoffmann forbidden, since they entail (2 + 2) or (4 + 4) cycloaddition. Formation of hexaprismane (**3**) from two benzene molecules is an even more unlikely triply forbidden reaction in that three orbital crossings occur along a D_{2h} reaction path. Thus, the species we study cannot be formed from ground-state benzene molecules by concerted symmetry-allowed pathways. This fact may enhance their interest because it means that if the species could be formed in some way, they would probably be quite stable. A $(CH)_6$ analogue of this is the Woodward–Hoffmann forbidden ground-state decay of Dewar benzene to benzene, which has a half-life of 2 days at room temperature. A nonconcerted pathway is also explored for the reaction **1** → **2**. There is precedent for the formation of dibenzene species **2**, since the anthracene dimer (**6**), containing a similar

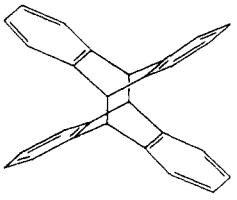

6

central moiety, has been synthesized photochemically and studied in the solid state.[2] Experiments at very high pressures (≃10 GPa = 100 kbars) also suggest the possibility of benzene dimer formation.[3] A consistent interpretation of the macroscopic high-pressure results can be made by assuming significant inter-ring overlap of the benzene π-electron orbitals,[4] although other interpretations have also been made which do not involve dimer formation.[5]

We used the semiempirical method MNDO[6] (modified neglect-of-diatomic-differential overlap) to explore the $(CH)_{12}$ energy surface and for coordinate optimizations. In some cases the calculations were augmented by a 2 × 2 configuration interaction (CI) within the MNDO scheme. In addition, ab initio GVB[7] and GVB–CI calculations based on GVB (generalized valence bond) orbitals have been carried out along some of the reaction paths determined by the MNDO procedure. The ab initio calculations sought (1) to address difficulties associated with a single Slater determinant wave function description of the Woodward–Hoffmann-forbidden reactions and (2) to give a more rigorous estimate of the changes in electron correlation energy which occur in the reactions. The relative energies of the various stable species examined were also calculated by using Benson's[8] thermochemical group-additivity method to further strengthen the conclusions.

The accuracy of MNDO, ab initio, and group-additivity descriptions of highly strained ring systems were tested by comparing to experimental heats of formation of benzene isomers and cyclobutane.

Details of the Calculations

MNDO Calculations. The technique used for determination of geometries and reaction paths was the semiempirical MNDO method,[6] in which the integrals for the Hartree–Fock calculations are retained at the neglect-of-diatomic-differential-overlap level. The MNDO procedure uses the core approximation, and molecular orbitals are approximated by the sum of a minimal basis set of valence-shell atomic orbitals. Optimizations on the energy hypersurface were accomplished by use of the finite-difference energy gradients and the Davidon–Fletcher–Powell algorithm. The calculations were begun by searching the $(CH)_{12}$ energy hypersurface with MNDO for stable points corresponding to inter-ring bonding. After finding the metastable structures, MNDO energy barriers to their formation from isolated benzenes were calculated along various reaction paths. For one reaction path, where biradical character was suspected, the double excitation from the highest occupied to lowest virtual orbital was included after the SCF calculation in a 2 × 2 MNDO CI calculation.

Ab Initio GVB and GVB–CI Calculations. To address the effects of orbital crossings and of changes in electron correlation effects along the reaction paths, the MNDO calculations were supplemented by ab initio generalized valence bond (GVB)[7] and CI calculations using the GVB orbitals. These calculations were carried out by using a minimal STO-3G basis of contracted gaussians on the C and H atoms. Instead of the normal single-configuration Hartree–Fock description, in which each electron pair is described by a doubly occupied orbital ϕ_1^2, we employed a GVB six-pair wave function with each of the six π-electron pairs replaced by a two-configuration expansion

$$C_1\phi_1^2 - C_2\phi_2^2$$

The Hartree–Fock wave function for two benzene molecules in D_{2h} symmetry is

$$\psi_{HF} = \Phi_\sigma\, 1b_{2u}^2 1b_{3u}^2 1a_g^2 1b_{3g}^2 1b_{2g}^2 1b_{1u}^2$$

whereas the GVB wave function is

$$\psi_{GVB} = \Phi_\sigma[1b_{2u},1a_u][1b_{3u},2b_{1u}][1a_g,2b_{2g}][1b_{3g},1b_{1g}] \times [1b_{2g},2a_g][1b_{1u},2b_{3u}]$$

Here, Φ_σ represents the doubly occupied orbitals of the σ-electron framework, and each term in brackets denotes a GVB pair, e.g.,

$$[1b_{2u},1a_u] = C_1 1b_{2u}^2 - C_2 1a_u^2$$

The pairing scheme was chosen (1) to describe smoothly the orbital crossings that occur among three of the electron pairs as two benzene molecules come together in D_{2h} symmetry (as will be discussed below) and (2) to describe the remaining orbital space that is spanned by the 12 π orbitals for carrying out the CI calculations.

(1) (a) This work was supported by the Department of Energy and by the Air Force Office of Scientific Research (under Contract AFOSR ISSA-82-00011). (b) Present address: Biological Sciences Research Center, Shell Development Co., Modesto, CA 95352.

(2) Ehrenberg, M. *Acta Crystallogr.* **1966**, *20*, 177.

(3) (a) Dick, R. D. *J. Chem. Phys.* **1970**, *52*, 6021; **1979**, *71*, 3203. (b) Engelke, R.; Hay, P. J.; Kleier, D. A.; Wadt, W. R. *Ibid.* **1983**, *79*, 4367. (c) Warnes, R. H. *Ibid.* **1970**, *53*, 1088.

(4) Pucci, R.; March, N. H. *J. Chem. Phys.* **1981**, *74*, 1373.

(5) Ree, F. H. *J. Chem. Phys.* **1979**, *70*, 974.

(6) (a) Dewar, M. J. S.; Thiel, W. *J. Am. Chem. Soc.* **1979**, *99*, 4899. (b) Thiel, W. *QCPE* **1979**, *11*, 379.

(7) (a) Goddard, W. A., III; Dunning, T. H., Jr.; Hunt, W. J.; Hay, P. J. *Acc. Chem. Res.* **1973**, *6*, 368. (b) Hay, P. J.; Hunt, W. J.; Goddard, W. A. III, *J. Am. Chem. Soc.* **1972**, *94*, 8293.

(8) Benson, S. W. "Thermochemical Kinetics"; Wiley: New York, 1976; Chapter 2.

Table I. MNDO *p,p'*-Dibenzene (**2**) and Hexaprismane (**3**) Geometries[a]

property[e]	*p,p'*-dibenzene[f] MNDO[b]	MINDO/3[c]	hexaprismane[g] MNDO[b]	MINDO/3[d]
point group	D_{2h}		D_{6h}	
interplane sepn, R	2.750	2.821	1.585	1.575
double C–C bond	1.353	1.354		
single C–C bond, within ring	1.528	1.536	1.548	1.560
single C–C bond, ring to ring	1.588	1.595	1.585	
angle C(1)C(9)C(4)	105.1		60.0	60
angle between the C(1)C(9)C(4) and C(1)C(2)C(3) planes	38.7		0.00	
CH bond C(1)–H(14)	1.088		1.097	1.110
CH bond C(9)–H(21)	1.112		1.097	1.110
angle C(11)C(9)C(21)	107.6		121.4	122
angle C(5)C(1)H(14)	111.9		121.4	122
angle C(2)C(1)H(14)	123.7		115.3	

[a] The MNDO benzene geometry has C–C and C–H bond lengths of 1.407 and 1.090 Å, respectively. [b] Present results. [c] Reference 9. [d] Reference 10. [e] Lengths in Å, angles in degrees. [f] Cf. Figure 1. [g] Cf. Figure 2.

Table II. Relative Energies (kcal/mol) of Dimeric Forms of Benzene As Computed by Various Methods[a]

method	relative energy, kcal/mol **1**[c]	**2**[d]	**3**[e]	**4**[f]	**5**[g]
MNDO	0	45	38	15	16
ab initio (STO-3G)					
HF	0	28	8	14	17
GVB	0	26	5		
GVB-CI ($10e^-$)	0	35	19		
GVB-CI ($12e^-$)	0	29	67		
group additivity	0[b]	41	95	52	52

[a] Zero-point vibrational energy changes are neglected. [b] $\Delta H_f = 39.6$ kcal/mol. [c] Two benzenes. [d] *p,p'*-Dibenzene. [e] Hexaprismane. [f] *exo-o,o'*-Dibenzene. [g] *endo-o,o'*-Dibenzene.

GVB–CI calculations were carried out in the space of the 12 π orbitals at two levels: (1) 12e–CI: all possible excitations were included among the 12 orbitals—this leads to a total of 28 236 spin eigenfunctions of ^1A_g symmetry in the D_{2h} point group. (2) $10e^-$CI: all possible excitations were included subject to the restriction that the $1b_{2u}$ orbital remain occupied and the $1a_u$ orbital remain unoccupied—this leads to only 2584 spin eigenfunctions.

In both the $12e^-$ and $10e^-$ CI calculations, at most eight open-shell orbitals could be present in the calculation.

Along the C_{2v} reaction path **2** → **1**, a GVB one-pair calculation was carried out in order to describe properly the orbital crossing that occurs along the path. This calculation is analogous to the MNDO 2 × 2 CI described above where the HOMO and LUMO are allowed to interact, except that in the GVB calculations the orbitals and mixing coefficients are all obtained self-consistently.

Group-Additivity Calculations. The thermochemical method of Benson,[8] which employs group additivities for bond heats of formation ($\Delta H_f°$) plus estimates of ring strain, was also used to obtain $\Delta H_f°$ values of the various stable species on the $(CH)_{12}$ surface. A discussion of these calculations is given in the Appendix.

Geometry Optimizations. The calculations were begun by searching the $(CH)_{12}$ energy hypersurface at the MNDO level for minima corresponding to stable points with inter-ring bonding. For species **2** and **3** all geometrical parameters were optimized in D_{2h} symmetry. The D_{2h} geometries of **2** and **3** were found to be unchanged when the point group constraint was relaxed to C_{2v}. This process was repeated for the **4** and **5** isomers in the C_{2h} and C_{2v} point groups, respectively. The energies and geometrical forms of species **2** through **5**, obtained in this way are given in Tables I–III and Figures 1–3.

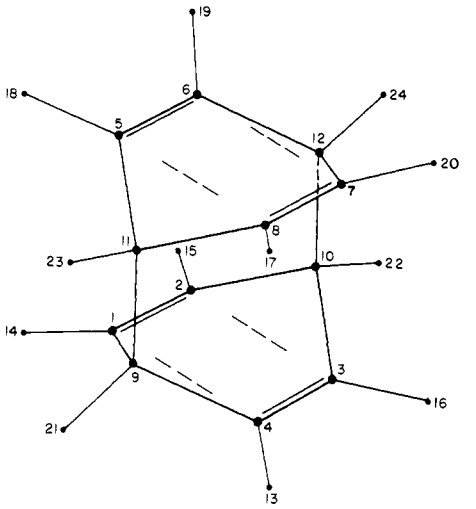

Figure 1. Scale perspective of the equilibrium (**2**) *p,p'*-dibenzene structure (D_{2h}). The carbon and hydrogen nuclei are labeled 1–12 and 13–24, respectively. This structure consists of two 1,4-cyclohexadiene rings held together by two σ bonds.

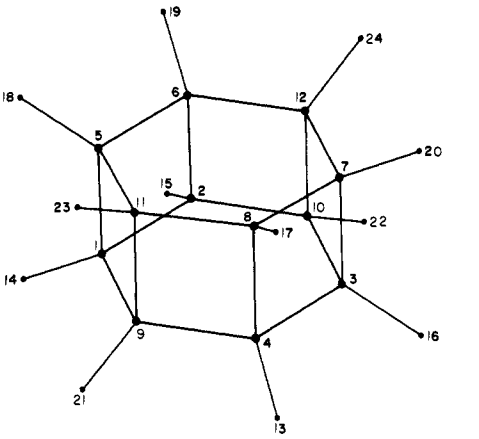

Figure 2. Scale perspective of the equilibrium (**3**) hexaprismane structure (D_{6h}). The carbon and hydrogen nuclei are labeled 1–12 and 13–24, respectively. This structure consists of two cyclohexane rings held together by six σ bonds.

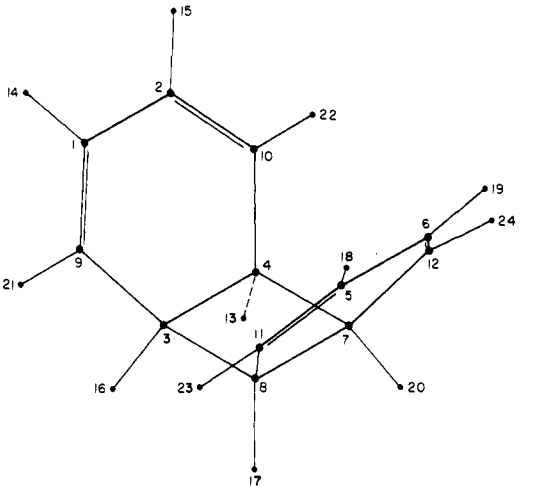

Figure 3. Scale perspective of the equilibrium (**5**) *endo-o,o'*-dibenzene structure (C_{2v}). The carbon and hydrogen nuclei are labeled 1–12 and 13–24, respectively. This structure consists of two 1,3-cyclohexadiene rings held together by two σ bonds.

D_{2h} Reaction Path for 1 → 2 → 3. The MNDO method was used to map out the reaction paths between the stable points on the $(CH)_{12}$ hypersurface. For the D_{2h} path corresponding to **1**

Table III. MNDO *o,o'*-Dibenzene Geometries[a]

bond lengths, Å		bond angles, deg		angles between planes, deg	
C(3)—C(8)	1.565	C(4)C(3)C(8)	90.0	C(8,3,4) and C(4,3,9)	56.6 (59.5)[b]
C(8)—C(11)	1.501	C(4)C(3)C(9)	115.9	C(4,3,9) and C(3,9,1)	1.1 (1.4)[b]
C(7)—C(8)	1.572	C(3)C(9)C(1)	122.5		
C(5)—C(6)	1.465	C(9)C(1)C(2)	121.6		
C(5)=C(11)	1.353				
C(8)—H(17)	1.113 (1.111)	C(8)C(3)H(16)	110.8 (112.9)	C(8,3,4) and H(16)C(3,8)	66.6 (66.2)[c]
C(11)—H(23)	1.091	C(3)C(9)H(21)	116.1	C(3,9,1) and H(21)C(9,3)	1.8 (1.4)[c]
C(5)—H(18)	1.091	C(9)C(1)H(14)	121.3	C(9,1,2) and H(14)C(1,9)	0.3 (1.5)[c]

[a] The point groups of the two species are endo (**5**) C_{2v} and exo (**4**) C_{2h}. Generally, only the endo properties are entered in the table. When endo and exo bond lengths (angles) are different by more than 0.001 Å (0.1°), the exo values are entered enclosed by parentheses. See Figure 3 for the definition of the numbering of the nuclei positions. C(*x*,*y*,*z*) indicates a plane containing nuclei *x*, *y*, and *z*. [b] Angles between carbon planes. [c] Angles for planes involving hydrogen nuclei.

→ **2** → **3**, four of the carbon nuclei in each benzene ring were forced to remain coplanar throughout the path (i.e., nuclei 1–4 and 5–8 of Figure 1), and the two planes so defined were parallel. The shortest distance between the planes was taken as the reaction coordinate (R). The remaining four carbon nuclei were not forced to remain coplanar with the other carbons of their ring but could move in any way consistent with the D_{2h} point group. The carbon and hydrogen nuclei of the two ring systems were in eclipsed position when viewed along the C_2 axis perpendicular to the carbon planes. There were three independent carbon–carbon bond distances (e.g., C(1)–C(2), C(1)–C(9), and C(9)–C(11) of Figure 1). The eight hydrogen nuclei attached to planar carbons were equivalent as were the four hydrogen nuclei attached to the four other carbons. There were two independent C–H bond lengths (e.g., C(1)–H(14) and C(9)–H(21) of Figure 1). The angles associated with the hydrogens were free within D_{2h} constraints. At large separation of the carbon planes, the point group of the system becomes D_{6h}. If this approach was continued for 2.75 Å $< R <$ 3.0 Å, one moved up a valley, the bottom of which lay higher in energy than nearby regions of the energy hypersurface. To circumvent this problem, the "flap" angles (e.g., the angle between the planes defined by C(5), C(8), C(6) and C(5), C(8), C(11) of Figure 1) were made to vary linearly with R from the R = 3.0 Å value to their value at structure **2** (R = 2.75 Å) during the energy optimization. This procedure leads out of the valley into the *p,p'*-dibenzene (**2**) minimum.

The D_{2h} reaction path leading from **2** to hexaprismane (**3**) was obtained by decrementing R by 0.1 Å or less, while minimizing the energy with respect to the free coordinates. No special procedures were necessary to reach the hexaprismane minimum at R = 1.59 Å.

A second D_{2h} reaction path leading from **1** to **2** was examined in which the reaction coordinate is the interplane C–C distance (C(9)–C(11) and C(10)–C(12)). For this path it was not necessary to impose any additional coordinate constraints other than the reaction coordinate. The MNDO energy barrier along this second D_{2h} path from **1** to **2**, however, is larger than that for the one described above.

C_{2v} Reaction Path for 1 → 2. A C_{2v} reaction path **1** → **2** was also investigated. The benzene rings were brought together so that one of the *p,p'*-dibenzene σ bonds forms earlier than the second. Thus, some bonding energy is obtained before the energy barrier to formation of the second bond is traversed. Figure 4 shows the C_{2v} structure after the first interplane σ bond has formed.

The C_{2v} reaction path had the following properties. On the entire path, carbons within the sets C(1) to C(4), C(5) to C(8), C(9) to C(12), and C(1), C(4), C(5), C(8) were coplanar. The C_2 rotation axis bisects and is perpendicular to the line connecting C(9) to C(11) and lies in the C(9)C(10)C(11) plane. There were five independent C–C bond lengths and four independent C–H bond distances. The bond angles were free within C_{2v} symmetry.

The C_{2v} path from **1** to **2** was as follows:

(I) Starting from **1**, the distance between the parallel lines defined by C(5)–C(8) and C(1)–C(4) was brought to the **2** value (2.75 Å).

(II) The angles of the two flaps defined by C(1), C(4), C(9) and C(5), C(8), C(11) were brought to their **2** values.

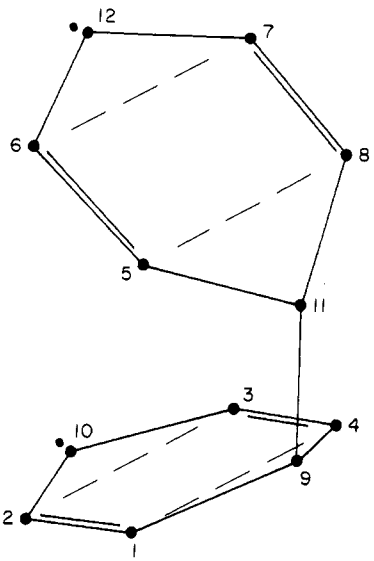

Figure 4. Scale perspective of a biradical structure on the C_{2v} reaction path leading to *p,p'*-dibenzene (**2**). This structure has one σ bond connecting two cyclohexadienyl radicals. Only the carbon nuclei are shown.

(III) The C–C bond lengths of the flap carbons of step II (e.g., C(1)–C(9)) were extended to their **2** values.

(IV) The separation of the parallel lines defined by C(2)–C(3) and C(6)–C(7) was brought to the **2** value.

(V) The flaps defined by C(2), C(3), C(10) and C(6), C(7), C(12) were brought to their **2** form. The final structure is (**2**) *p,p'*-dibenzene.

In this procedure, after a coordinate was brought to its **2** value, it was fixed for the remainder of the reaction path. All the coordinates not fixed in this way were optimized, within the C_{2v} symmetry constraint, to give the minimum energy.

C_{2v} and C_{2h} Reaction Paths for 1 → 5 and 1 → 4. On the C_{2v} reaction path for **1** → **5**, the four carbon nuclei C(3), C(4), C(7), and C(8) were forced to form a rectangle (see Figure 3). The reaction coordinate (R) was the shortest distance between the parallel lines defined by C(3)–C(4) and C(7)–C(8). Five distinct C–C bond lengths were possible (e.g., C(7)–C(8), C(8)–C(3), C(8)–C(11), C(11)–C(5), and C(5)–C(6) of Figure 3). Three distinct C–H bond lengths were allowed (e.g., C(8)–H(17), C(11)–H(23), and C(5)–H(18) of Figure 3). The angles were free within the constraints of the C_{2v} point group. For the endo (**5**) form, the angle between the planes defined by C(3)C(4)C(9) and C(7)C(8)C(11) was less than 180°.

For the C_{2h} reaction path for **1** → **4** (*exo-o,o'*-dibenzene), all the statements for the endo path apply, except the angle between the planes defined by C(3)C(4)C(9) and C(7)C(8)C(11) of Figure 3 was fixed at 180°.

Results and Discussion

Orbital Considerations. If one considers the π orbitals of two benzene molecules (**1**) along the D_{2h} reaction path to *p,p'*-dibenzene (**2**) and thence to hexaprismane (**3**), the schematic orbital

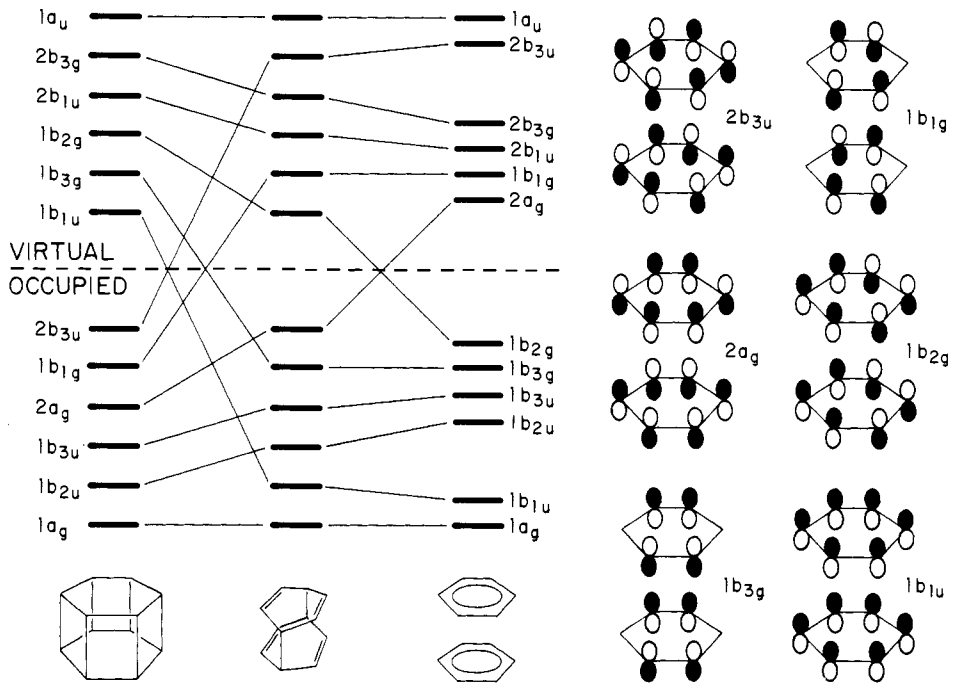

Figure 5. Schematic molecular orbital correlation diagram along the D_{2h} dimerization path.

correlation diagram shown in Figure 5 is obtained. The two sets of a_{1u} and e_g π orbitals on each benzene molecule produce the ($1a_g$,$1b_{1u}$) and ($1b_{2u}$,$1b_{3u}$,$1b_{3g}$,$1b_{2g}$) orbitals, respectively, for two interacting C_6H_6 molecules in the reduced D_{2h} symmetry. Similarly the e_u and b_{2g} π^* orbitals of benzene yield the virtual ($2a_g$,$1b_{1g}$,$2b_{1u}$,$2b_{3g}$) and ($2b_{3u}$,$1a_u$) orbitals shown in the figure.

Formation of the two inter-ring σ bonds requires a crossing between the occupied $1b_{2g}$ and virtual $2a_g$ orbitals, since the former orbital is antibonding between the rings, while the latter orbital is bonding in character. In the GVB calculations, therefore, the [$1b_{2g}$,$2a_g$] pair is able to allow the smooth change in configuration from $(1b_{2g})^2$ to $(2a_g)^2$ along the reaction path for this Woodward–Hoffmann forbidden (4 + 4) addition.

Similarly, hexaprismane formation along the D_{2h} path requires an orbital crossing between two pairs of orbitals—[$1b_{1u}$,$2b_{3u}$] and [$1b_{3g}$,$1b_{1g}$] shown in Figure 5. These pairs are treated in an equivalent manner to the previous orbital pair by the GVB procedure. The remaining π^* orbitals, which remain formally unoccupied for this reaction, are obtained by arbitrary pairings with the occupied orbitals as discussed in the section on calculational details.

Stable Dimers of Benzene. We first consider local minima on the hypersurface corresponding to metastable $(CH)_{12}$ isomers. Two forms corresponding to face-to-face chemically bound benzene dimers were found—*p,p'*-dibenzene (**2**), tricyclo[4.2.2.$2^{2,5}$]dodeca-3,7,9,11-tetraene, with an interplane carbon separation of 2.75 Å, and hexaprismane (**3**), heptacyclo-[6.4.0.$0^{2,7}$.$0^{3,6}$.$0^{4,11}$.$0^{5,10}$.$0^{9,12}$]dodecane, with an interplane separation of 1.59 Å. The structural parameters for both molecules are given in Table I. The numbering of the nuclei is that used in Figures 1 and 2. The bond lengths and angles, which are similar to the values derived earlier by Dougherty, Schlegel, and Mislow[9] for **2** and Minkin and Minyaev[10] for **3** using MINDO/3 calculations, reflect normal C–C single and double bond lengths. Compounds **2** and **3** were still found to be metastable when the point group was relaxed to C_{2v}.

If we compare the relative stabilities (see Table II) of these species, MNDO predicts **2** and **3** to be comparable in energy but thermodynamically unstable relative to two benzenes (**1**) by 38 and 45 kcal/mol, respectively. The most extensive GVB–CI calculations place hexaprismane (**3**) at higher energy (67 kcal/mol) than *p,p'*-dibenzene (**2**) (29 kcal/mol), relative to two ground-state benzene molecules (taken as 0 kcal/mol). The latter ordering is also in accord with the group additivity estimates (see Appendix) of the relative stabilities of **3** (95 kcal/mol) and **2** (41 kcal/mol). While the theoretical methods all give relatively consistent energies for **2**, the MNDO, HF, and GVB procedures, apparently, overestimate the stability of **3**. The GVB–CI ($12e^-$) hexaprismane energy is significantly nearer the thermochemical estimate than are other quantum-mechanical results. We shall return to this point in the next section.

Table IV. Heats of Reaction (kcal/mol) for $2C_2H_4 \rightarrow C_4H_8$

method	basis set	geometries	ΔH_f	ref
experiment			−18.7	11
group additivity			−18.6	8
MNDO	minimal	optimized	−42.6	this work
HF	STO-3G	optimized	−79.1	12a
HF	STO-3G	from MNDO	−79.9[b]	this work
GVB–CI	STO-3G	from MNDO	−36.9[c]	this work
HF	4-31G	optimized	−13.6	12b,c
HF	DZ[a]	from MNDO	−14.3[d]	this work
GVB–CI	DZ[a]	from MNDO	+10.9[e]	this work

[a] DZ = (9s5p/4s)/[3s2p/2s] from: Dunning, T. H., Jr.; Hay, P. J. In "Modern Theoretical Chemistry"; Schaefer, H. F., III, Ed., Plenum Press: New York, 1977; Vol. III. [b] $E[2(C_2H_4)]$ = −154.14416 hartrees; $E(C_4H_8)$ = −154.27156 hartrees. [c] $E[2(C_2H_4)]$ = −154.23228 hartrees; $E(C_4H_8)$ = −154.29102 hartrees. [d] $E[2(C_2H_4)]$ = −156.02155 hartrees; $E(C_4H_8)$ = −156.04428 hartrees. [e] $E[2(C_2H_4)]$ = −156.08074 hartrees; $E(C_4H_8)$ = −156.06329 hartrees.

The *o,o'*-dibenzene species (**4** and **5**), *exo*- and *endo*-tricyclo-[6.4.0.$0^{2,7}$]dodeca-3,5,9,11-tetraene, were also found to correspond to local energy minima (see Table II) on the $(CH)_{12}$ hypersurface. Their structural parameters are given in Table III. These isomers have stabilities comparable to **2**—about 10 kcal/mol less stable according to group additivity estimates but about 30 kcal/mol more stable according to MNDO.

Assessment of Thermochemical Stabilities. Since most of the $(CH)_{12}$ isomers are considerably strained (with the possible exception of **2**), one can ask whether the theoretical estimates are providing reliable energies for these systems. There are at least two studies of interest—(1) comparing two C–C double bond energies with the energy of a strained four-member ring system

(9) Dougherty, D. A.; Schlegel, H. B.; Mislow, K. *Tetrahedron* **1978**, *14*, 1441.
(10) Minkin, V. I.; Minyaev, R. M. *Zh. Org. Khim.* **1981**, *17*, 221.
(11) Benson, S. W.; O'Neal, H. E. "Kinetic Data on Gas Phase Unimolecular Reactions"; NSRDS-NBS21: Washington, 1970; p 269.

Table V. Relative Energies (kcal/mol) of C_6H_6 Isomers

isomer	MNDO	HF,[a] STO-3G	expt	group additivity
7, benzene (D_{6h})	0.0	0.0	0.0	0.0
8, benzvalene (C_{2v})	80.4	72.5	<91.2	69.4
9, Dewar benzene (C_{2v})	68.1	79.0	59.5	72.1
10, triprismane (D_{3h})	100.7	95.3	91.2	102.6

[a] Calculated at the MNDO optimized geometries.

(e.g., $2C_2H_4 \rightarrow C_4H_8$) and (2) comparing the energies of various $(CH)_6$ isomers.

Table IV compares various calculated heats of reaction for $2C_2H_4 \rightarrow C_4C_8$ to experiment. All the calculations (including MNDO) which employ minimal basis sets significantly overestimate the stability of the strained four-membered ring of cyclobutane. Earlier Pople and co-workers[12a] considered the isodesmic reaction, $2C_2H_4 \rightarrow C_2H_2 + C_2H_6$, and demonstrated that STO-3G basis sets provide a poor description of the π bond in ethylene. This problem is ameliorated by using double-ζ (DZ) bases, which can describe the carbon 2p orbitals involved in σ and π bonds equivalently (cf. Table IV). There is also a significant differential electron correlation error between the π bonds of the two ethylenes and the two new σ bonds of cyclobutane. The GVB–CI is designed to reduce this error, leading to a better description of the two ethylenes. The DZ HF calculations give fortuitously good heats of reaction, while the DZ GVB–CI calculations actually lead to the wrong sign for the heat of formation. Polarization basis functions are needed to describe the strained four-membered rings in cyclobutane properly and to obtain a good heat of reaction.

The results in Table IV indicate that both the MNDO and STO-3G GVB–CI calculations should overestimate the stability of hexaprismane with its six four-membered rings relative to two benzenes. The $(CH)_{12}$ results support this conclusion (see Table II) since hexaprismane (**3**), which possesses six such rings, lies 7 kcal/mol lower than dibenzene at the MNDO level, 38 kcal/mol higher at the GVB–CI (12e$^-$) level, compared with 54 kcal/mol higher using thermochemical group additivities, which may be high by 10–20 kcal/mol (cf. Appendix). For the *o,o'*-dibenzenes (**4** and **5**), with one four-membered ring, the MNDO results are about 35 kcal/mol lower than the group additivity estimates. Note that one cannot make a quantitative correction to the MNDO *o,o'*-dibenzene energy by use of the error in the MNDO energy for cyclobutane.

For the isomers benzene (**7**), benzvalene (**8**), Dewar benzene (**9**), and triprismane (**10**), a similar comparison can be made

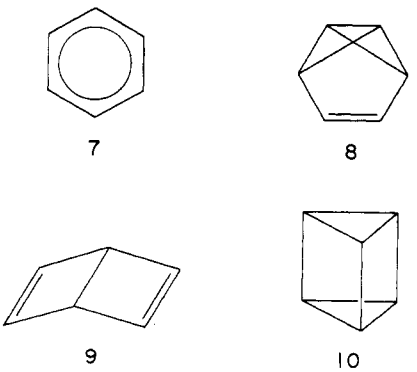

between strained ring systems, since experimental results for heats of isomerization are available.[13] It is of interest in the comparison that Dewar benzene (**9**) and triprismane (**10**) bear a resemblance to *p,p'*-dibenzene (**2**) and hexaprismane (**3**), respectively. In Table V, quantum mechanical, group-additivity, and experimental results

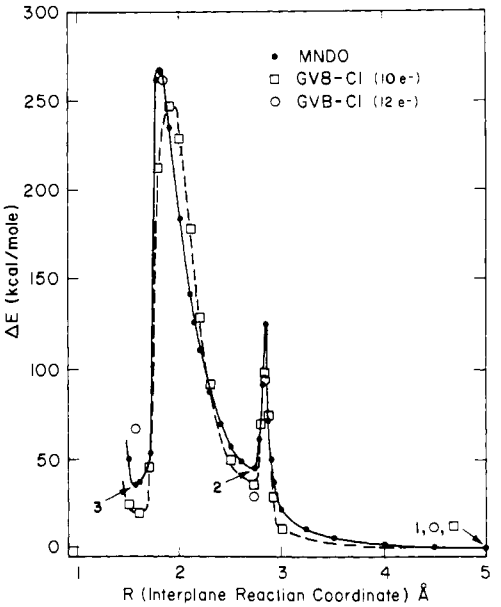

Figure 6. MNDO and GVB energies along the D_{2h} reaction path leading from **1** → **2** → **3**.

Table VI. Barriers to Formation Relative to Two Benzene Molecules As Computed from Various Methods

method	barrier to formation, kcal/mol[a] 2	3	4	5
MNDO	127 (D_{2h})[b] 161 (C_{2v})	265 (D_{2h})	159 (C_{2h})	127 (C_{2v})
2 × 2 MNDO CI	97 (C_{2v})			
ab initio, STO-3G				
GVB	130 (D_{2h})	275 (D_{2h})		
GVB–CI (10e$^-$)	97 (D_{2h})	247 (D_{2h})		
GVB–CI (12e$^-$)	95 (D_{2h})	264 (D_{2h})		

[a] Relative to two benzenes. [b] Point group symmetry enforced along the reaction path.

for the energies of **7**–**10** are compared. The MNDO energies correspond to fully optimized geometries within the indicated point groups. The HF energies were evaluated at the MNDO geometries in order to parallel the procedure used in calculating the dimer energies. The experimental energies are for structures that were fully methylated; in the calculations, we neglected any alteration in the heats of isomerization due to the presence of methyl groups rather than hydrogens.

The agreement of the various energies for these strained systems is superior to what would be expected from the $2C_2H_4 \rightarrow C_4H_8$ analysis given above. The group-additivity energies are in good agreement with the MNDO values except for benzvalene (**8**). For **9** and **10** both MNDO and group-additivity energies are high relative to experiment by about 10 kcal/mol. The scatter in the minimal set HF results is somewhat worse than for the other methods.

We do not understand why the energies given by the various techniques are in better agreement for these smaller strained systems than they are for the dimers. The agreement of the various results for **10** is perplexing because this system contains three cyclobutane rings, for which MNDO is known to give inferior results. An unquestioning acceptance of the benzene isomer results would suggest MNDO energy errors of about ±20 kcal/mol for systems as large as **2**–**5**.

Reaction Barriers. We first consider the D_{2h} reaction path from **1** to **2** to **3** in which the interplane separation (defined by the four carbon nuclei which remain planar in each ring) defines the reaction coordinate (R) shown in Figure 6. Along this path, distinct barriers (arising from the orbital crossings discussed above) exist between each of the three isomers. The barriers (see Table VI) appear more cusp-like in the single-determinant MNDO calculations than in the GVB calculations, where the wave function

(12) (a) Lathan, W. A.; Hehre, W. J.; Pople, J. A. *J. Am. Chem. Soc.* **1971**, *93*, 808. (b) Hehre, W. J.; Pople, J. A. *Ibid.* **1975**, *97*, 6941. (c) Cremer, D. *Ibid.* **1977**, *99*, 1307.

(13) Oth, J. F. M. *Agnew Chem., Int. Ed. Engl.* **1968**, *7*, 646.

Table VII. CI Coefficients from GVB Calculations along the D_{2h} Reaction Path

	pair 1		pair 2		pair 3	
R, Å	$1b_{2g}$	$2a_g$	$1b_{3g}$	$1b_{1g}$	$1b_{1u}$	$2b_{3u}$
3.0[a]	0.9968	0.0805	0.9968	0.0802	0.9999	0.0161
2.93	0.9961	0.0881	0.9967	0.0817	0.9999	0.0169
2.87	0.9932	0.1167	0.9965	0.0831	0.9998	0.0193
2.84[b]	0.2406	0.9706	0.9977	0.0677	0.9995	0.0324
2.81	0.1004	0.9949	0.9977	0.0678	0.9992	0.0389
2.75[c]	0.0430	0.9991	0.9975	0.0671	0.9988	0.0485
2.50	0.0364	0.9993	0.9972	0.0754	0.9986	0.0531
2.30	0.0321	0.9995	0.9958	0.0914	0.9981	0.0618
2.20	0.0300	0.9995	0.9942	0.1080	0.9975	0.0702
2.10	0.0280	0.9936	0.9902	0.1396	0.9964	0.0847
2.00	0.0261	0.9997	0.9737	0.2279	0.9925	0.1195
1.90	0.0245	0.9997	0.1257	0.9921	0.1592	0.9872
1.80[b]	0.0224	0.9297	0.0725	0.9974	0.0721	0.9974
1.70	0.0235	0.9997	0.0365	0.9993	0.0330	0.9995
1.60[d]	0.0217	0.9998	0.0275	0.9996	0.0254	0.9997
1.50	0.0201	0.9998	0.0213	0.9998	0.0200	0.9998

[a] Benzene (**1**). [b] Transition state. [c] *p,p*-Dibenzene (**2**). [d] Hexaprismane (**3**).

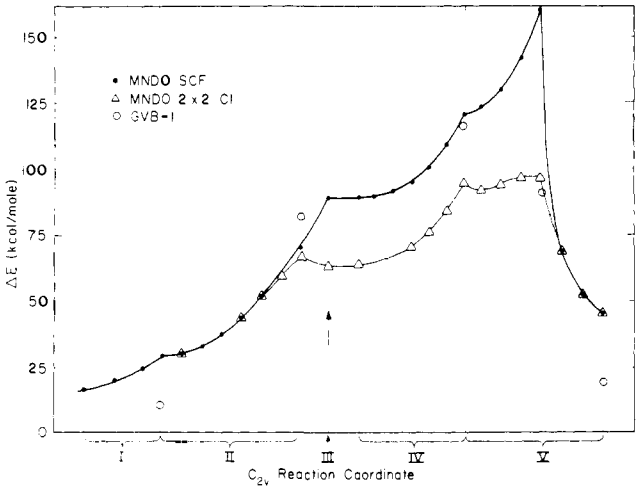

Figure 7. MNDO, MNDO 2 × 2 CI, and GVB–CI energies along the C_{2v} reaction path leading from **1** → **2**. The roman numerals on the figure correspond to parts of the reaction coordinate described in the text. In particular, the point denoted by III corresponds to the structure shown on Figure 4.

passes smoothly between the configurations involved in the orbital crossings. The weighting coefficients of these configurations from GVB calculations are given in Table VII; the changes of configuration are observed to be quite abrupt along the reaction coordinate.

The calculated barriers to interconversion of these species (Table VI) are sufficiently high—95 kcal/mol between **1** and **2**, 264 kcal/mol between **3** and **1**, and 235 kcal/mol between **2** and **3**—to make the kinetic stability of these species likely, if there are no significantly lower energy decomposition routes. For the second D_{2h} reaction path from **1** to **2** described above (where R = C-(9)–C(11)), a MNDO reaction barrier of 139 kcal/mol is obtained; this is higher by 12 kcal/mol than that for the first D_2h path. It is interesting that the energy barrier between **2** and **3** is roughly twice that between **1** and **2**; i.e., the energy barrier corresponding to the process involving two orbital crossings is about twice that for the one with one crossing. This may mean that there are lower symmetry paths between **2** and **3**, on which the orbital crossings occur separately, which are of significantly lower energy.

An alternate reaction path was explored for the reaction **1** → **2**, where a lower symmetry C_{2v} path between **1** and **2** was also studied (Figure 4). The C_{2v} reaction path was defined in a somewhat arbitrary manner. The resulting C_{2v} cut on the potential energy surface (Figure 7) is not a significantly lower energy pathway to decomposition than the D_{2h} path. MNDO 2 × 2 CI calculations at the MNDO geometrical coordinates produced a still large, but significantly reduced, reaction barrier on the C_{2v} path. Ab initio calculations using a two-configuration GVB-1 wave function also produced a large reaction barrier (≃120 kcal/mol) along the MNDO D_{2v} path.

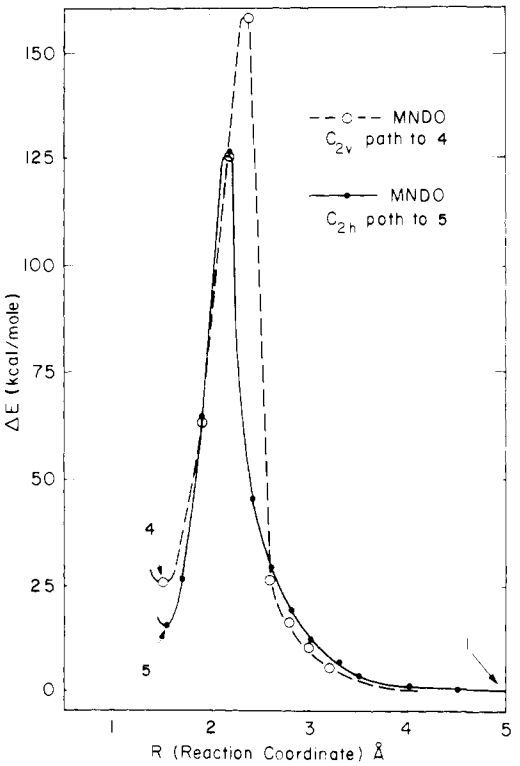

Figure 8. MNDO energies along the C_{2h} and C_{2v} reaction paths from **1** → **4** and **1** → **5**.

Concerted addition of two benzenes to form the *o,o'*-dibenzene molecules (**4** and **5**) also leads (Figure 8) to high-activation barriers (130–160 kcal/mol) as expected for a Woodward–Hoffmann forbidden (2 + 2) cycloaddition.

Comments on Experimental Synthesis of the Dimers

Numerous chemically bound $(CH)_{12}$ structures have been synthesized.[14] To our knowledge only species **5** of those considered here has been experimentally isolated.[15] Attempts at synthesis of **2** have been made; these resulted in a structure close to but not the desired one.[16] It is possible that **2** has been produced in

(14) (a) Scott, L. T.; Jones, M., Jr. *Chem. Rev.* **1972**, *72*, 181 and references therein. (b) Greenberg, A.; Liebman, J. F. "Strained Organic Molecules"; Academic Press: New York, 1978; p 214 and references therein.
(15) (a) Oth, J. F. M.; Rottele, H.; Schroder G. *Tetrahedron Lett.* **1970**, No. 1, 61. (b) Berson, J. A.; Davis, R. F. *J. Am. Chem. Soc.* **1972**, *94*, 3658.

very high-pressure shock-wave experiments.[3a,b] However, this is not certain because of the difficulty of making microscopic observations in such experiments. An important aspect of the shock-wave work is that for every arene experimentally tested,[3a,c] one finds the same evidence of a possible dimerization process. Therefore, the dimerization mechanism leading to **2** may apply to arene systems in general.

The calculated high barriers along the reaction coordinates for **2**, **3**,and **4** → **1** suggest that these species may be experimentally realizable. In this regard, it is important that the calculated barriers are also spatially wide as this prevents disintegration to **1** by tunneling. It is of interest that cubane (**11**) has been synthesized[17] and that it is as highly strained as the most strained structure we consider (**3**). Application of the group additivity

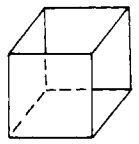

11

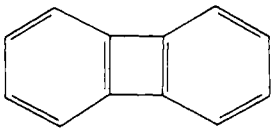

12

method to **11** and **3** indicates that the ring strain for both of these systems is about +160 kcal/mol. Thus, the strain energies of **2**, **3**, and **4** alone may not preclude their existence.

Finally, biphenylene (**12**), which is quite close in structure to the *o,o'*-dibenzenes (**4**, **5**), was synthesized long ago[18] and may be a reasonable place to start a synthesis route to some of the structures considered here. It does not seem to have been used as a precursor molecule in the synthesis paths used to date.

It may be possible to produce excited electronic states of the dimers by photochemically exciting one of the reacting benzene molecules; such processes could be Woodward–Hoffmann allowed and thus would avoid the large reaction barriers of the ground-state reactions. Relaxation of the excited dimer to its ground electronic state would, perhaps, yield one the structures studied in this paper.

Appendix: Thermochemical Group-Additivity Calculations

For the strained ring structures considered in this paper, the group-additivity estimate of the heat of formation is

$$\Delta H_f^\circ(\text{ring}) = \sum_i \Delta H_f^\circ(\text{bond})_i + \sum_j \Delta H_f^\circ(\text{strain})_j$$

where ΔH_f°(ring) is the heat of formation estimate for the ring, $\Delta H_f^\circ(\text{bond})_i$ is the contribution to the heat of formation for the bonding characteristic of the i^{th} carbon, and $\Delta H_f^\circ(\text{strain})_j$ is a correction corresponding to the ring strain of the j^{th} small ring in the larger structure. The advantage of this procedure is that information on only a small number of bond classes and on the strain energy for a few small ring systems allows one to compute ΔH_f° values for many complex ring structures.

As an example of this approach, consider triprismane (**10**) for which the ΔH_f° estimate is

$$\Delta H_f^\circ(\mathbf{10}) = 6\Delta H_f^\circ[\text{C}-(\text{C})_3(\text{H})] + 3\Delta H_f^\circ[\text{cyclobutane}] + 2\Delta H_f^\circ[\text{cyclopropane}]$$

When numerical values[8] are entered in this equation, one finds $\Delta H_f^\circ(\mathbf{10})$ = 122.4 kcal/mol. The strain terms contribute +133.8 kcal/mol and therefore are critically important in obtaining an accurate ΔH_f° estimate. When the measured heats of formation[13] for hexamethyltriprismane are compared, this approach overestimates the strain energy by 15%. Similar errors are found for the strain energy in hexamethyl(Dewar benzene). Hence, the thermochemical estimates for *p,p'*-dibenzene (**2**) should be accurate to ±5 kcal/mol (small strain energy), while those for hexaprismane (**3**) may be high by 20 kcal/mol.

In the case of **2**, we had to estimate two of the ΔH_f° contributions using values in ref 8. These were (1) the bond contribution for the interring σ bonds, where we used

$$\Delta H_f^\circ[\text{C}-(\text{C}_d)_2(\text{C})(\text{H})] \simeq \Delta H_f^\circ[\text{C}-(\text{C}_d)_2(\text{H})_2] + \Delta H_f^\circ[\text{C}-(\text{C}_d)(\text{C})_2(\text{H})] - \Delta H_f^\circ[\text{C}-(\text{C}_d)(\text{C})(\text{H})_2] \simeq -1.01 \text{ kcal/mol}$$

and (2) the ring-strain contribution for the two 1,5-cyclooctadiene rings in **2**, where we used

$$\Delta H_f^\circ[\text{1,5-cyclooctadiene}] \simeq (1/2)[\Delta H_f^\circ(\textit{cis}\text{-cyclooctene}) + \Delta H_f^\circ(\text{1,3,5-cyclooctatriene})] \simeq +7.5 \text{ kcal/mol}$$

Using this approach, we obtained the group-additivity estimates given in Tables II, IV, and V.

There are some shortcomings in the group-additivity technique in application to our systems. For example, in computing the ring-strain energy contribution of the two cyclohexane rings in **3**, we used Benson's value of 0 kcal/mol. This value corresponds to nonplanar equilibrium cyclohexane. However, the cyclohexane rings in **3** are planar. Similarly, the inter-ring C–C single bonds in **4** are not of standard length, yet we use a ΔH_f° contribution corresponding to a standard single C–C bond. These simplifications must result in some inaccuracies in the estimates. Further, it is also important to realize that the group-additivity method, at present, is only applicable to equilibrium structures, and hence cannot give information on system energy at general points on a reaction path (e.g., at a transition state).

Registry No. 1, 6842-25-7; **2**, 69122-64-1; **3**, 4493-26-9; **4**, 21657-71-6; **5**, 91279-91-3; C_2H_4, 74-85-1.

(16) Yang, N. C.; Neywick, C. V.; Srinivasachar, K. *Tetrahedron Lett.* **1975**, No. 49, 4313.
(17) (a) Eaton, P. E.; Cole, T. W., Jr., *J. Am. Chem. Soc.* **1964**, *86*, 962. (b) Fleischer, E. B. *Ibid.* **1964**, *86*, 3889.
(18) Lothrop, W. C. *J. Am. Chem. Soc.* **1941**, *63*, 1187; **1942**, 64, 1698.